Radiative Properties of Eastern Pacific Stratocumulus Clouds

Zach Pecenak, Evan Greer, Changfu Li

Section 1: Introduction

The reality that ongoing climate change exists is the primary impetus for unconventional solutions such as climate engineering. As a complement to reducing humanity's carbon footprint, climate engineering manipulates the climate itself to counteract warming and other global issues. Solar radiation management techniques (SRM) is a form of climate engineering that attempts to adjust the amount of radiation received at the surface by controlling radiation and heat reflected to space. (Corner and Pidgeon, 2010). Understanding the properties of clouds is a key to the development of effective solar radiation management techniques.

Evaluation of the effect of clouds on heating rates and the thermodynamic balance within the Earth's atmosphere needs to be effectively addressed before any SRM methods can be employed. Clouds drive radiative forcing within the atmosphere by reflecting shortwave radiation and absorbing longwave radiation. The study of the interaction of clouds with the atmospheric radiative balance is complicated by the variety of spatial scales associated with individual clouds and cloud systems as well as the differences between cloud types. (Curry and Webster, 1998)

Marine stratocumulus clouds have served as the focus in many studies involving the effect of cloud properties on radiative forcing. Marine stratocumulus clouds are accompanied by significant changes radiative fluxes. (Nicholls, 1984) Marine stratocumulus clouds form persistently in the Eastern Pacific where the interaction of warm dry air interacts with the cold ocean surface. (Lu et al, 2007) The turbulent mixing of fog or stratus layers drives the formation of stratocumulus clouds. (Curry and Webster, 1998) The effect of aerosol perturbations, caused by the passing of ships, on marine stratocumulus in the Eastern Pacific has shown measurable effects on local climates. (Lu et al., 2009) In this study, we investigate how the droplet distribution of a marine stratocumulus cloud determines the cloud properties using to study radiative forcing.

Section 2: Description of the Radiative Model

The model uses the inputs of a measured cloud droplet distribution $n(r)$ from an eastern Pacific marine stratocumulus cloud (Lu et al. 2009). The data was extracted into Matlab using DataThief in the form of a data file. From the given data several properties of the clouds could be inferred.

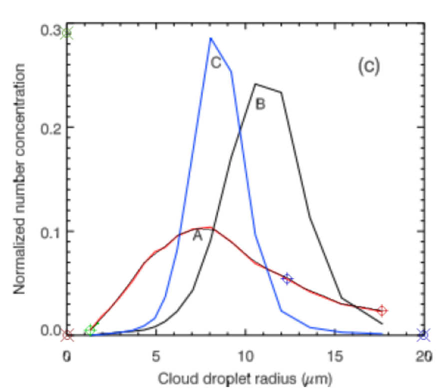

Figure 1: Droplet distribution from Lu. et al. The read curve was taken as the distribution for an "undisturbed" cloud

From a given distribution profile, the total number concentration of particles per cm^3can be found by

$$N = \int_0^\infty n(r)dr \approx \sum n(r) \tag{1}$$

Since the distribution is numerical the equation can be simplified to a summation. Following the total number concentration the liquid water mixing ratio (w_l) is found using the definition. w_l is a measure of the mass of liquid water mixed into dry air and is important in both precipitation and radiative processes.

$$w_l = \frac{M_{lw}}{M_{da}} = \frac{\rho_l}{\rho_a}\frac{4}{3}\pi \int_0^\infty r^3 n(r)dr \tag{2}$$

Where the density of liquid is measured in grams and the density of air is measures in kg, thus giving units of g/kg. The liquid water mixing ratio is used to find the liquid water path of the clouds. The liquid water path is a measure of the density of the path electromagnetic radiation must travel through to reach the surface. This is defined as the integral of the mixing ratio from the base to the top of the cloud.

$$Wl = \int_{Z_{cb}}^{Z_{ct}} \rho_a\, w_l dz \tag{3}$$

Two convenient measures of describing the size of the droplets from the given distribution are the mean radius and the effective radius. The mean radius of the clouds is simply the mathematical average of the distribution of the droplet radii and is given by the following formula.

$$\bar{r} = \frac{\int_0^\infty n(r)rdr}{\int_0^\infty n(r)dr} \approx \frac{n\ \cdot r}{N} \tag{4}$$

The effective radius is essentially a measure of the mean radius that is weighted by the cross section of the droplets. Due to the nature of the weighting, that cross section varies as r^2, the larger drops have a higher weighting and $r_e > \bar{r}$. This measure is given by the form,

$$r_e = \frac{\int_0^\infty n(r)r^3 dr}{\int_0^\infty n(r)r^2 dr} \tag{5}$$

From Mie theory, the solution of Maxwell's equations introduces several coefficients which describe the extinction of radiation through a cloud. The extinction coefficient is essentially a measure of the light that is either scattered or absorbed through a cloud. This value is defined in the following manner.

$$\sigma_{ext} = \pi \int_0^\infty r^2 n(r)dr\, Q_{ext}(\lambda)dr \tag{6}$$

Since the wavelength is solar, the extinction efficiency Q_{ext} can be approximated as 2. The extinction coefficient is important in determining the optical depth of the cloud. The optical depth is a measure of resistance to light traveling through a cloud and is related to the absorptivity of the cloud through Beer's law. The optical depth is defined as

$$\tau_{ext} = \int \sigma_{ext} dz = \frac{3Wl}{2\rho_l r_e} \tag{7}$$

Since the data is numerical, all of the integrals are calculated numerically using Simpsons rule. A sensitivity analysis was performed to determine the effect of the changing the droplet concentration on all of the properties. By varying the distribution from 0 to 100 times its original value, a relationship between the concentration and all of the above introduced properties can be gained. The results of this analysis are discussed in the final section.

The code then evaluates the radiative properties of the same cloud type as measured from a DC-8 aircraft (Hayasaka et. All 1995, Nicholls 1984). From the data, a radiative balance is used to determine values of reflectivity, absorptivity, and transmissivity of the clouds to solar flux. This is done through a solution to a system of equations balancing the incoming and outgoing flux into the cloud. It should be noted that a black body assumption is not used in the analysis.

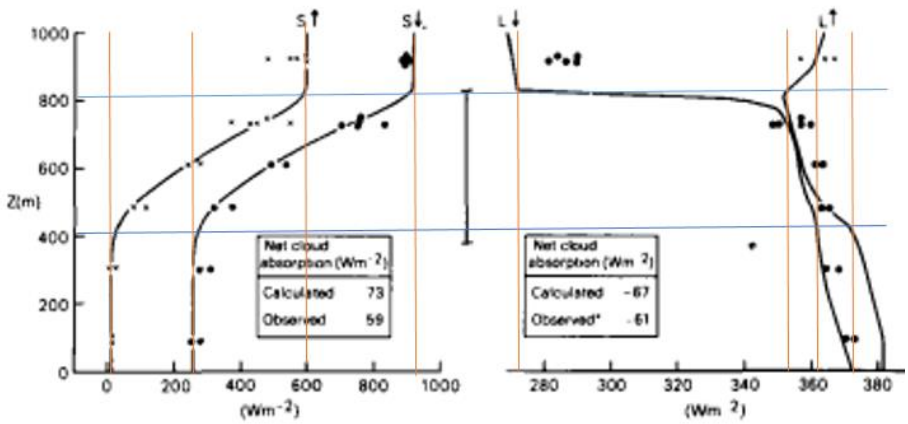

Figure 2Longewave radiation balance from Nicholls (1984). The blue lines represent the cloud top and bottom. The orange lines represent the flux values.

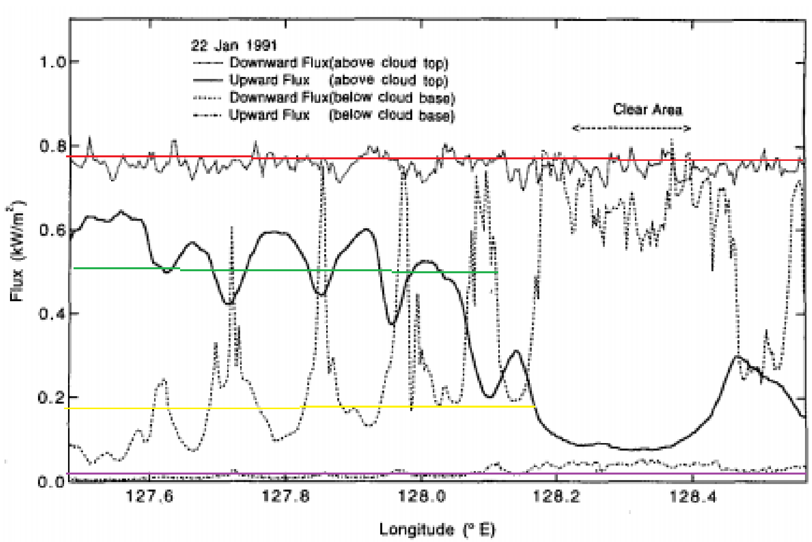

Figure 3: The solar flux as measured by Hayasaka et al 1985. The colored lines represent the average of each of the measured fluxes.

From the Longwave Flux, the emissivity of the cloud is determined from equation 3 from Stevens (1978). Using the radiative fluxes, the heating rate for both long wave and shortwave radiation can be found. This is found using equations 3.32 and 3.35 from Curry and Webster (1998).

$$\frac{dT}{dt} = \frac{1}{\rho c_p}\frac{dF}{dz} \approx \frac{1}{\rho c_p}\frac{\left(F_{net,ct} - F_{net,cb}\right)}{z_{ct} - z_{cb}} \tag{8}$$

The heating rate is given in terms of temperature per time and has units of kelvins/day. A positive heating rate indicates a warming effect as where a negative heating rate indicates a cooling effect. To compare the heating rate of the eastern Pacific marine stratocumulus cloud with another cloud, a sample radiative flux from Curry and Webster (1998) for arctic stratus was also calculated. The comparison is made in the conclusion section.

The model makes several assumptions and has a few possible shortcomings. The model assumes that the measured distribution is accurate and a proper representation of the total cloud. For the numerical integration Simpsons rule is used for simplicity and could be a large source of error. Similarly, the reader should understand that the measurements are from the same type of cloud, not the identical cloud. In fact the measured shortwave and long wave flux are measured in different parts of the pacific, thus possibly leading uncoupled results. However, the assumption is made that the pacific stratocumulus are similar enough that they can be correlated.

Section 3: Results and Discussion

A sensitivity study was performed by changing the droplet concentration and keeping the particle size distribution same in order to investigate the effect of varying droplet radius distribution on cloud properties important to the atmospheric radiative balance. A series of number distributions was generated as depicted in figure 4. From the sensitivity analysis, the Volume Extinction Coefficient increases linearly with the concentration. This indicates with more droplets, radiation will extinct faster when transferring through the cloud. This agrees well with the results of the cloud optical depth. As exceed the radius properties (effective and mean) did not change with changing concentration.

The radiative properties of the Eastern Pacific Stratocumulus (EPMS) and Arctic Stratus (AS) were determined from cloud properties and measured solar fluxes and compared. The determined cloud properties, solar flux measurements and heating rates are tabulated in table 1. Positive heating rate means the cloud is being heated by the absorption of shortwave radiation while negative sign means the cloud is being cooled by emission of longwave radiation.

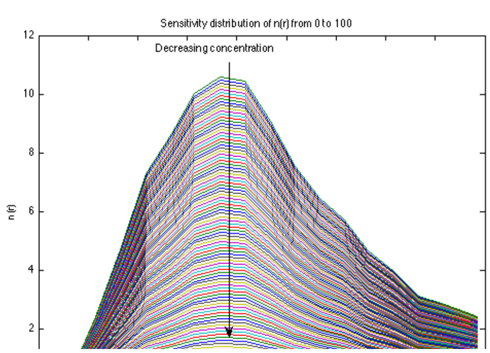

Figure 4: Sensativity analysis study. Vary the concentration from 0 to 100 times the original.

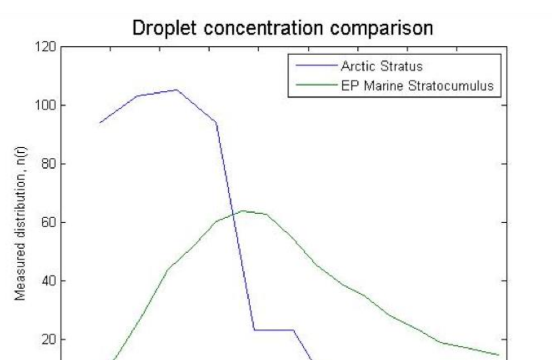

Figure 5: Droplet distribution comparison between Arctic Stratus and Eastern Pacific Stratocumuls

	Arctic Stratus		Marine Stratoculmus	
Solar Flux	Downward	Upward	Downward	Upward
	595	399	870	500
	337	187	185	30
Longwave Flux	Downward	Upward	Downward	Upward
	235	328	280	375
	326	331	361	376
Transmissivity	0.395		0.193	
Reflectivity	0.547		0.568	
Absorbtivity	0.059		0.268	
Solar Heating Rate	39.5		59.9	
Longwave Heating Rate	-11.2		-12.5	

Table 1: Comparison of radiative results between EPMS and AS

Accounting for the temperature of the cloud with Wien's displacement law, the radiation emitted by the cloud is longwave while solar radiation is shortwave, so we can draw the conclusion that the cloud absorbs shortwave energy from the sun which causes heating and emits longwave radiation which causes cooling. The AS cloud by comparison to the EPMS has a lower temperature and exists in a lower humidity environment. So the decreased heating rate agrees with the expected physics of the two clouds. It's interesting that heating rate is related to the transmission of the cloud, specifically, higher heating rate is related to larger liquid water path, which indicates larger optical depth. And larger optical depth means less transmission. This is in accord with the results we get by calculation, comparing to AS, EPMS has higher heating rate and lower transmissivity at the same time.

From figure 5, we can see EPMS has larger droplets and larger concentration than AS, so it can be inferred that EPMS is thicker cloud compared. From table 1, we know transmissivity, reflectivity, and absorbtivity for Arctic Stratus are 0.395, 0.547, and 0.059 respectively, for EPMS are 0.193, 0.568 and 0.268 respectively. Therefore, EPMS have lower transmissivity, higher reflectivity and higher absorbtivity than AS, this means less radiation will reach earth surface if we have EPMS other than AS. Combined analysis above, a conclusion can be reached that droplets distribution affects radiative properties of clouds directly. Increasing particle size and decreasing distribution might be an effective radiation management scheme to combat surface warming..

In this study, we investigated changing droplet concentration in clouds, and the corresponding effect on radiation transfer. We found that radiation balance is dependent on the cloud properties, i.e. droplet size and concentration. Heating rate is coupled with liquid water path, which will affect radiation transmission through the cloud. Finally, we found manipulating droplets distribution maybe a good way to do radiation management to cool the earth.

References:

Corner, Adam, and Nick Pidgeon (2010) Geoengineering the Climate: The Social and Ethical Implications, Environment: Science and Policy for Sustainable Development, 52: 1, 24-37, DOI: 10.1080/00139150903479563

Curry, Judith A., and Peter J. Webster. *Thermodynamics of atmospheres and oceans*. Vol. 65. Academic Press, 1998.

G. L. Stephens, 1978: Radiation Profiles in Extended Water Clouds. II: Parameterization Schemes. *J. Atmos. Sci.*, 35, 2123–2132. doi: http://dx.doi.org/10.1175/1520-0469(1978)035<2123:RPIEWC>2.0.CO;2

Lu, M., et al. (2007), The Marine Stratus/Stratocumulus Experiment (MASE): Aerosol-cloud reationships in marine stratocumulus. J. Geophys. Res., 112, D10209, doi:10.1029/2006JD007985

Lu, M.-L., A. Sorooshian, H. H. Jonsson, G. Feingold, R. C. Flagan, and J. H. Seinfeld (2009), Marine stratocumulus aerosol-cloud relationships in the MASE-II experiment: Precipitation susceptibility in eastern Pacific marine stratocumulus, J. Geophys. Res., 114, D24203, doi:10.1029/2009JD012774.

Nicholls, S. (1984), The dynamics of stratocumulus: Aircraft observations and comparisons with a mixed layer model. Q.J.R. Meteorol. Soc., 110: 783–820. doi: 10.1002/qj.49711046603

Tadahiro Hayasaka, Nobuyuki Kikuchi, and Masayuki Tanaka, 1995: Absorption of solar radiation by stratocumulus clouds: aircraft measurements and theoretical calculations. *J. Appl. Meteor.*, 34, 1047–1055.

Contents

Group ZEC

Problem 5

```
clc;
clear all;

%Givens
dr=1.5;
DelimeterIn=',';
C=(1:100)';
dat=importdata('nr.dat',DelimeterIn);
r=dat.data(:,1); %um

for j=1:length(C)
```

```
n(:,j)=dat.data(:,2)*C(j); %#/cm^3
rhoa=1.293; %kg/m^3
rhol=1000; %kg/m^3
z=300; %m
```

Part a

```
%Number concentration (summ of all counts)
N(j)=sum(n(:,j));
% fprintf('\ntotal number concentration is = %0.1f per cubic cm\n',N(j))

%liquid water mixing ratio
WL=0;
%r is converted to cm (r(i)*10^-3)
%rhol is converted to g
for i=1:length(r)-1
        WL=WL+((1/6)*((r(i)*10^-3)^3)*((r(i+1)-r(i))*10^-3)*(n(i+1,j)+n(i,j)+2*(n(i+1,j)+n(i,
j))));
end
```

```
wl(j)=WL*((rhol*1000)/rhoa)*(4/3)*pi;
% fprintf('\nThe liquid water mixing ratio is = %0.3f g per kg\n',wl(j))

%Mean drop size
rbar(j)=dot(n(:,j),r)/N(j);
% fprintf('\nThe mean drop size radius is = %0.3f um \n',rbar(j))

%Effective radius
reT=0;
reb=0;
for i=1:length(r)-1

        reT(i)=(1/6)*(r(i)^3)*(r(i+1)-r(i))*(n(i+1,j)+n(i,j)+4*(0.5*(n(i+1,j)+n(i,j))));
        reb(i)=(1/6)*(r(i)^2)*(r(i+1)-r(i))*(n(i+1,j)+n(i,j)+4*(0.5*(n(i+1,j)+n(i,j))));

end
re(j)=sum(reT)/sum(reb);
% fprintf('\nThe effective radius is = %0.3f um \n',re(j))

%volume extinction coefficient
rexT=0;
for i=1:length(r)-1
rexT(i)=(1/6)*(r(i)^2)*2*pi*(r(i+1)-r(i))*(n(i+1,j)+n(i,j)+4*(0.5*(n(i+1,j)+n(i,j))));
end
Sig_ext(j)=sum(rexT)*10^-6;
% fprintf('\nThe volume extinction coefficient is = %0.3f um^-1 \n',Sig_ext)
```

Part b

```
Wl(j)=z*rhoa*wl(j);
% fprintf('\nThe liquid water path is = %0.3f g/m^2 \n',Wl(j))
```

Part c

```
Tau_ext(j)=3000*Wl(j)/(2*rhol*re(j));
% fprintf('\nThe cloud optical depth is = %0.3f \n',Tau_ext(j))
```

```
end

%Plotting time
figure(1)
plot(r,n)
title('Sensitivity distribution of n(r) from 0 to 100')
xlabel('r (\mum)')
ylabel('n(r)')
annotation(figure(1),'arrow',[0.460714285714286 0.460714285714286],...
        [0.85952380952381 0.223809523809524]);
annotation(figure(1),'textbox',...
        [0.324214285714284 0.819047619047622 0.322214285714287 0.0952380952380976],...
        'String',{'Decreasing concentration'},...
        'FitBoxToText','off',...
        'LineStyle','none');
```

```
figure(2)
plot(C,N)
title('Sensitivity Number Concentration N from concentration 0 to 100')
xlabel('Concentration')
ylabel('N_c (cm^-^3)')

figure(3)
plot(C,wl)
title('Sensitivity mixing ratio w_l from concentration 0 to 100')
xlabel('Concentration')
ylabel('w_l g/kg')

figure(4)
plot(C,rbar)
title('Sensitivity mean Radius from concentration 0 to 100')
xlabel('Concentration')
ylabel('Mean Radius (\mum)')

figure(5)
plot(C,re)
title('Sensitivity Effective Radius from concentration 0 to 100')
xlabel('Concentration')
ylabel('Effective Radius r_e (\mum)')

figure(6)
plot(C,Sig_ext)
title('Sensitivity volume extinction coefficient from concentration 0 to 100')
xlabel('Concentration')
ylabel('Volume Exctinction coefficient')

figure(7)
plot(C,Wl)
title('Sensitivity Liquid water path from concentration 0 to 100')
xlabel('Concentration')
ylabel('Liquid water path(g/m^2)')

figure(8)
plot(C,Tau_ext)
title('Sensitivity cloud optical depth from concentration 0 to 100')
xlabel('Concentration')
ylabel('cloud optical depth, \tau')
```

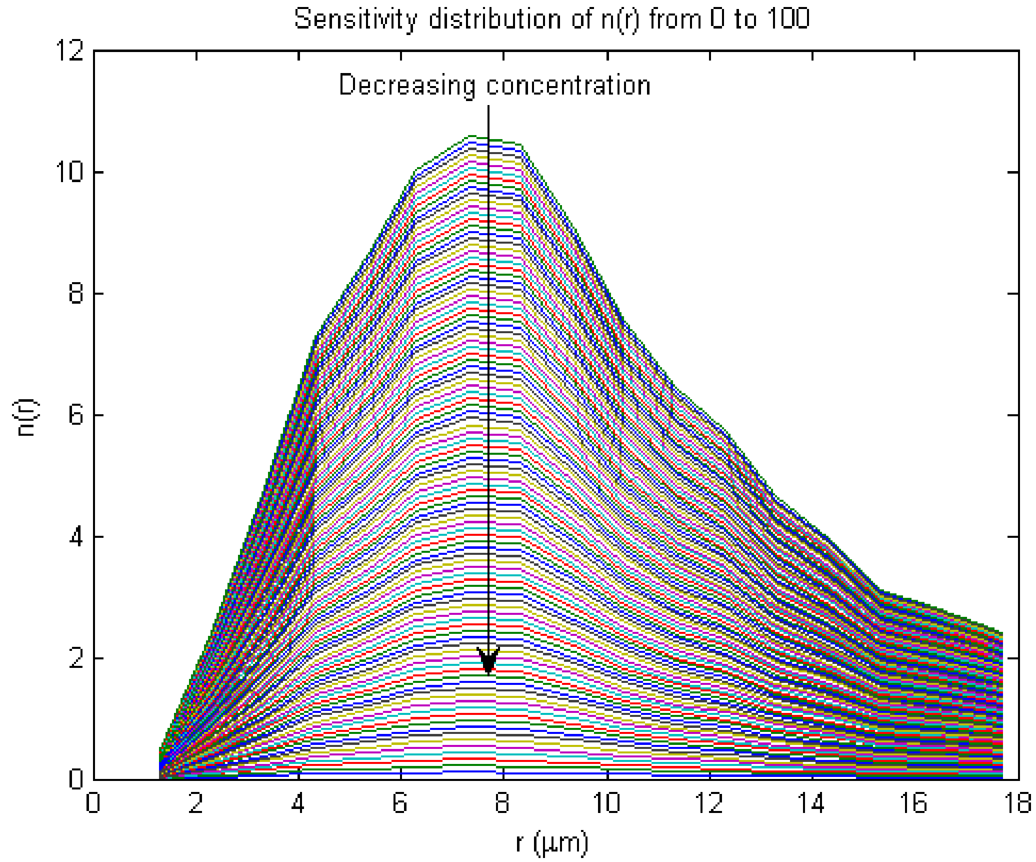
Sensitivity distribution of n(r) from 0 to 100
Decreasing concentration
n(r)
r (μm)
0
2
4
6
8
10
12
14
16
18

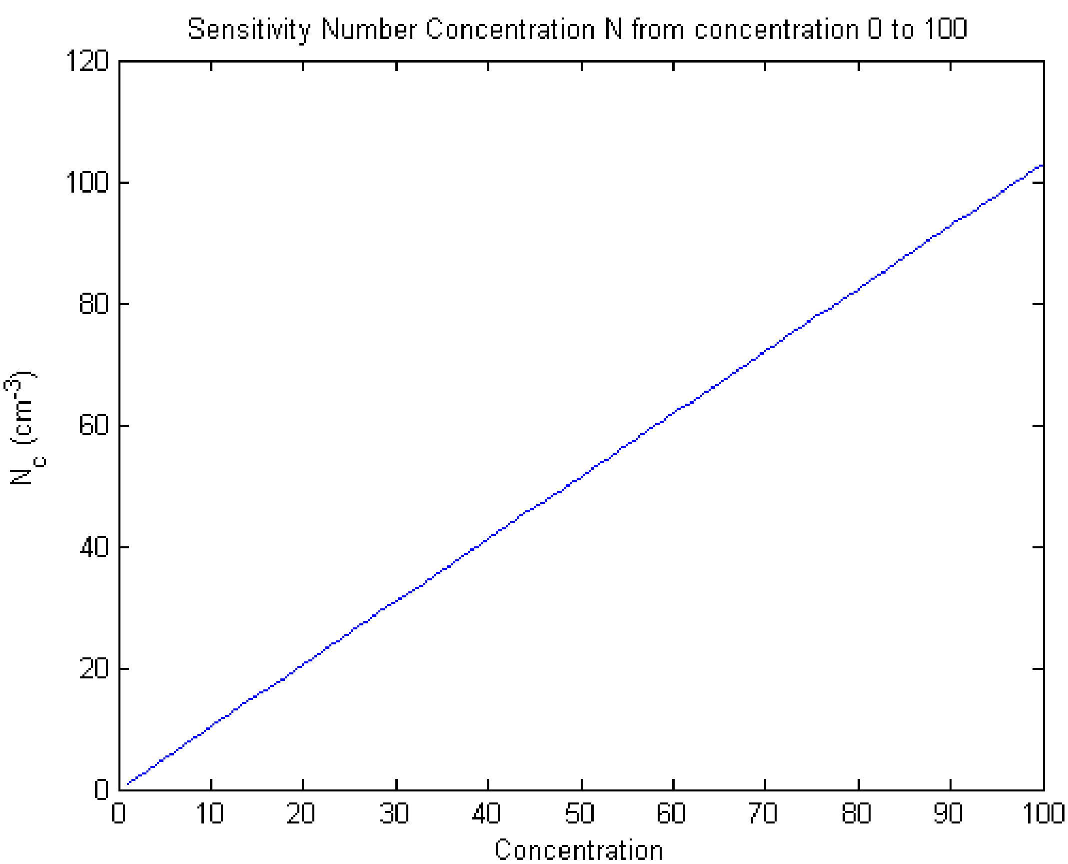
Sensitivity Number Concentration N from concentration 0 to 100
N_c (cm^-3)
Concentration
0
10
20
30
40
50
60
70
80
90
100
120

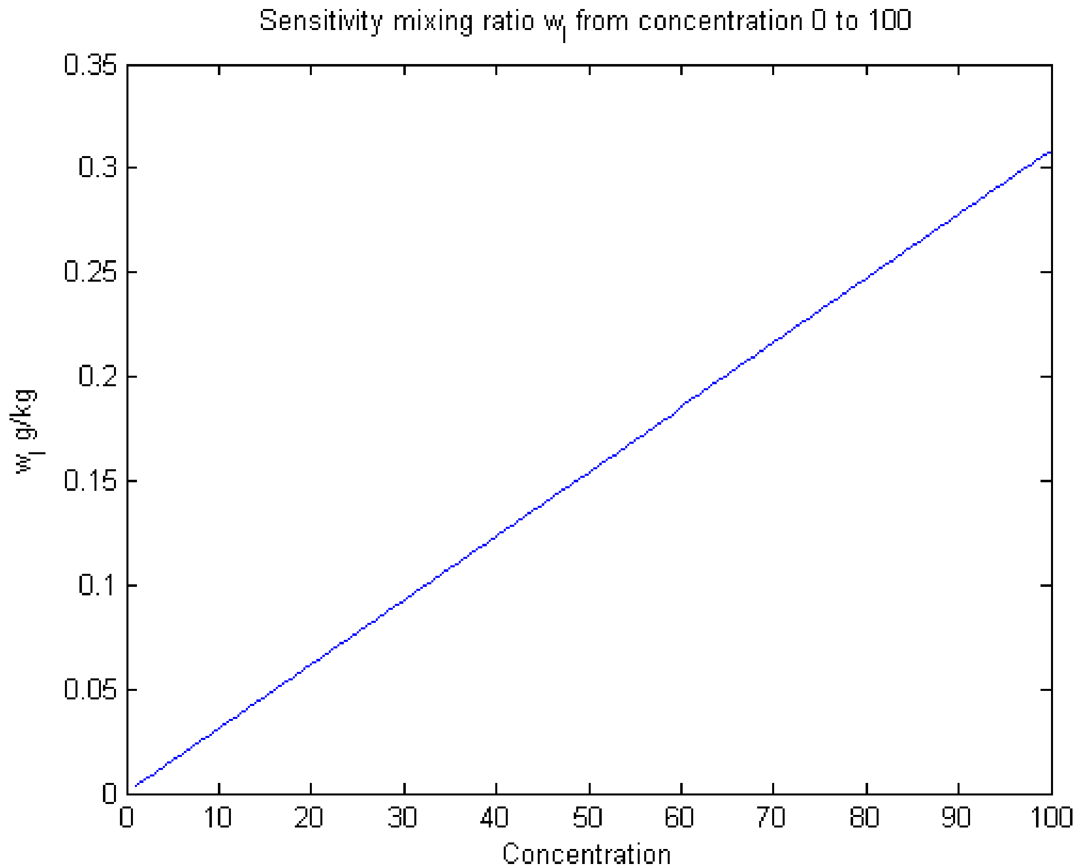
Sensitivity mixing ratio w_l from concentration 0 to 100
0.35
0.3
0.25
0.2
0.15
0.1
0.05
0
0
10
20
30
40
50
60
70
80
90
100
Concentration
w_l g/kg

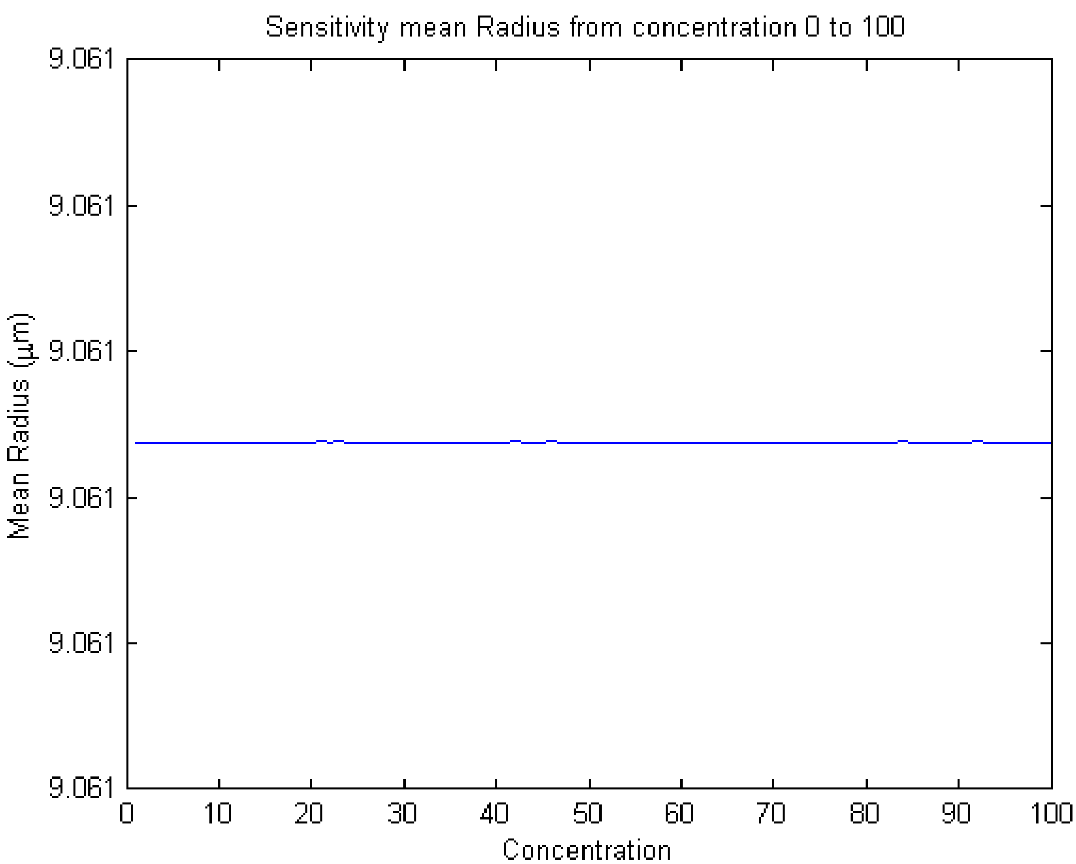
Sensitivity mean Radius from concentration 0 to 100
9.061
9.061
9.061
9.061
9.061
9.061
0
10
20
30
40
50
60
70
80
90
100
Concentration
Mean Radius (μm)

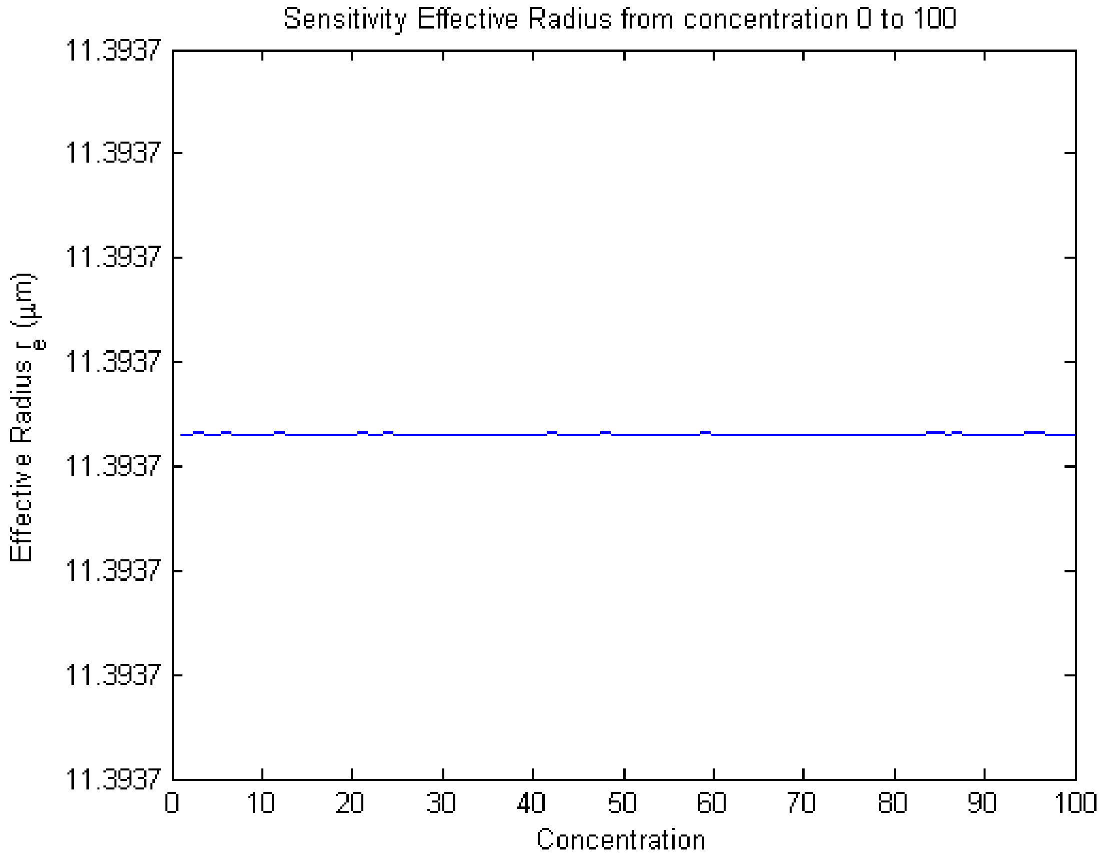
Sensitivity Effective Radius from concentration 0 to 100
11.3937
11.3937
11.3937
11.3937
11.3937
11.3937
11.3937
11.3937
Effective Radius r_e (μm)
0 10 20 30 40 50 60 70 80 90 100
Concentration

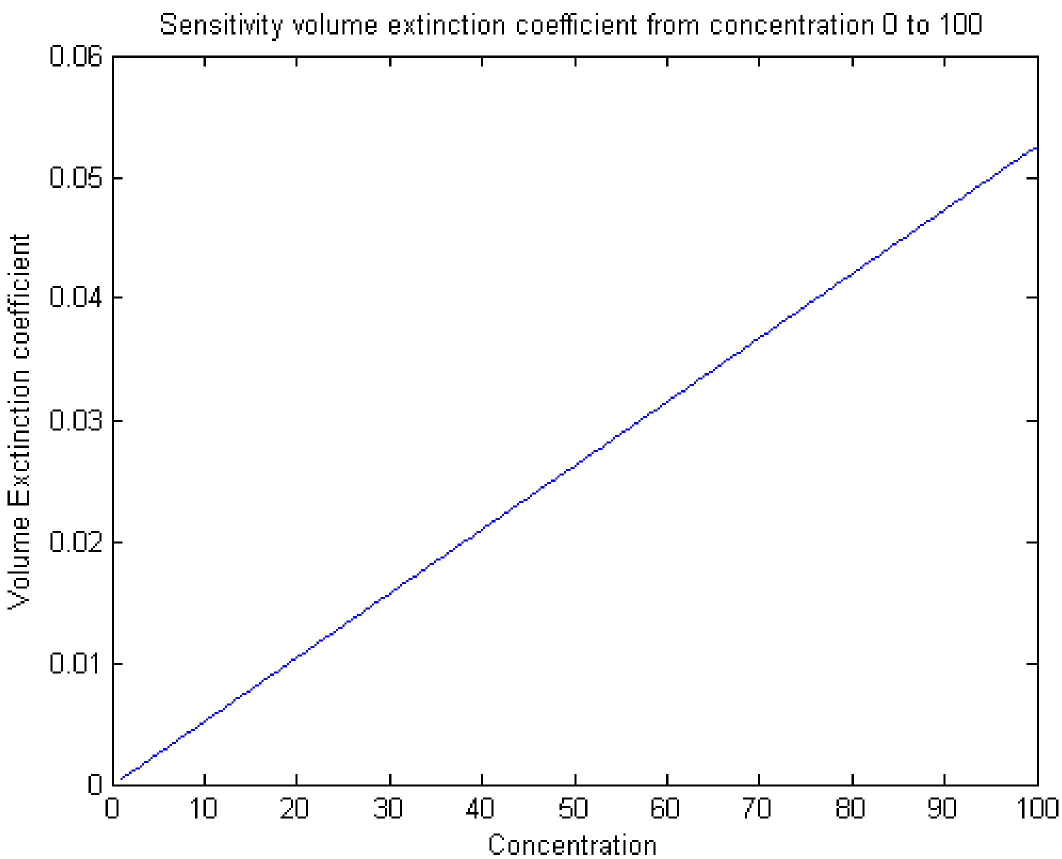
Sensitivity volume extinction coefficient from concentration 0 to 100
0.06
0.05
0.04
0.03
0.02
0.01
0
Volume Exctinction coefficient
0 10 20 30 40 50 60 70 80 90 100
Concentration

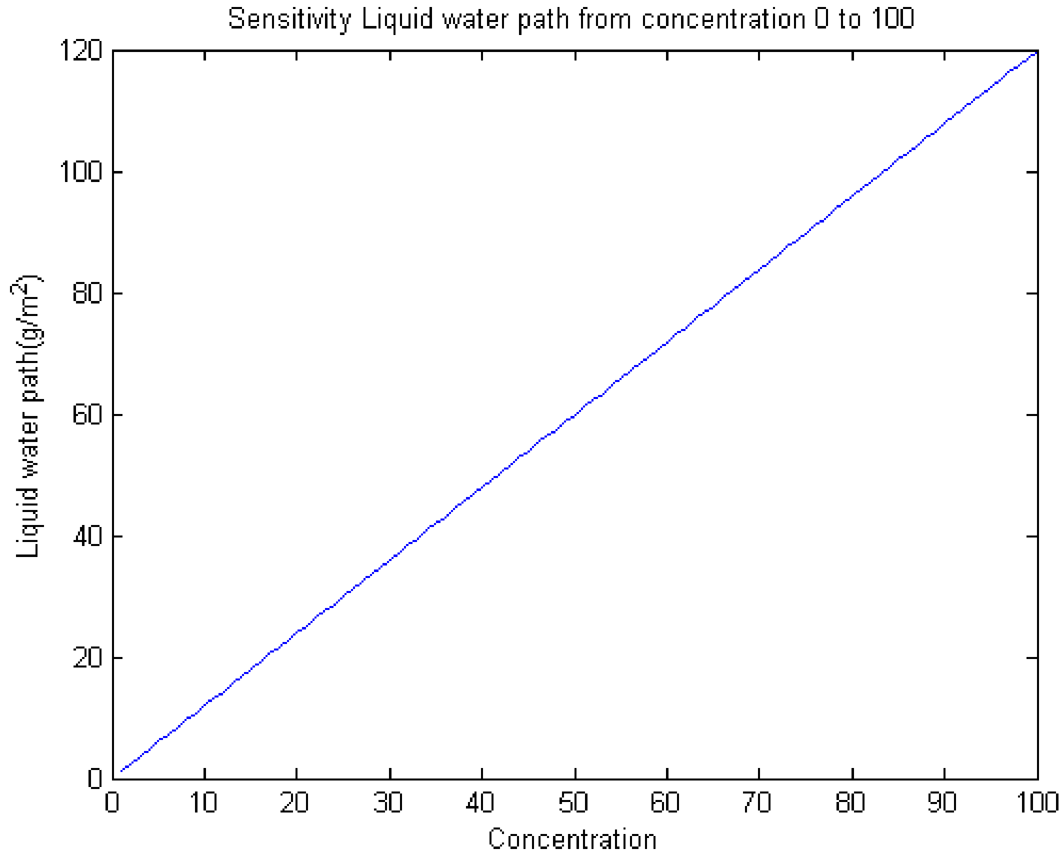
Sensitivity Liquid water path from concentration 0 to 100
Liquid water path(g/m^2)
Concentration
0
20
40
60
80
100
120
0
10
20
30
40
50
60
70
80
90
100

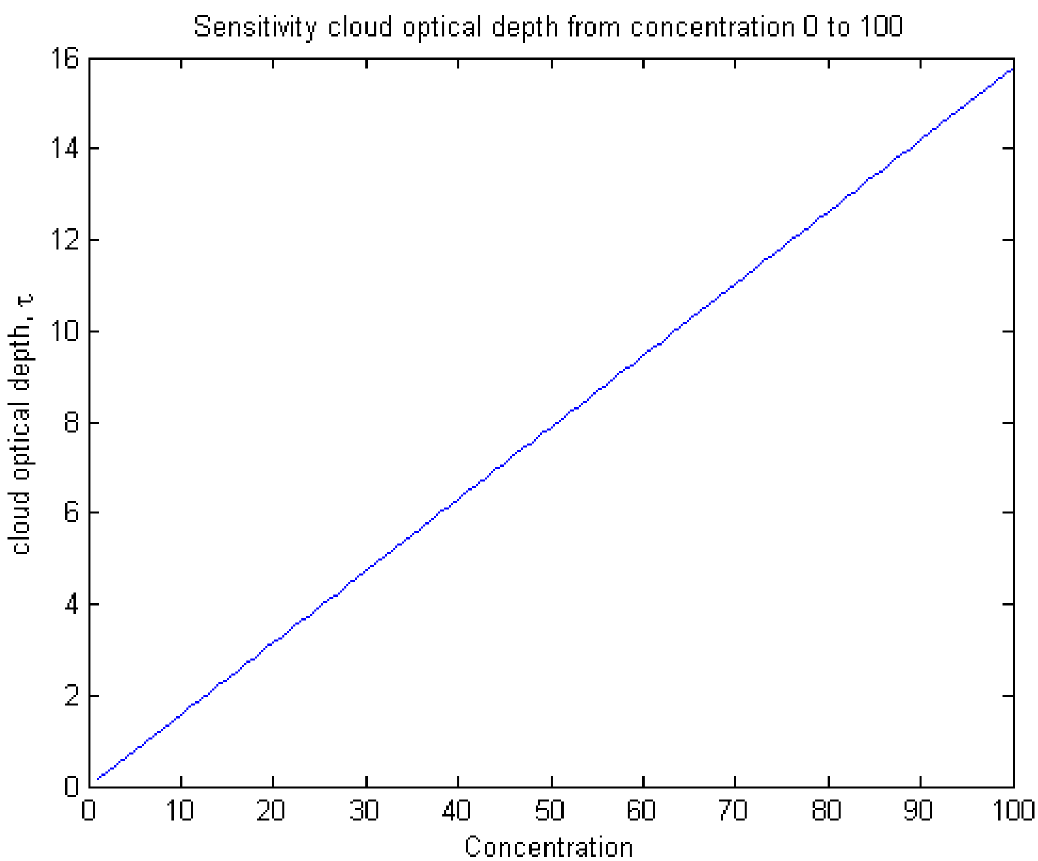
Sensitivity cloud optical depth from concentration 0 to 100
cloud optical depth, τ
Concentration
0
2
4
6
8
10
12
14
16
0
10
20
30
40
50
60
70
80
90
100

Part b)

```
%Givens
Cb=350; %m
Ct=800; %m
CT=307; %K
Sa=0.58;
rhoa=1.293; %kg/m^3
rhol=1000; %kg/m^3
z=300; %m
cp=1952; %J/kgK

%Flux
SctD=595;
SctU=399;
ScbD=337;
ScbU=187;
LctD=280;
LctU=375;
LcbD=361;
LcbU=376;
```

Part a)

```
%Transmissivity,Reflect,absorb
M=[1 1 1; SctD ScbU 0;  ScbU SctD 0;];
b=[1 ScbD SctU]';

x=inv(M)*b;
T=x(1);
R=x(2);
A=x(3);
fprintf('\nT is = %0.3f, R is = %0.3f, A is = %0.3f\n',T,R,A)
```

```
T is = 0.395, R is = 0.547, A is = 0.059
```

Part b)

```
Ro=(R-Sa*T^2)/(1-(Sa^2)*T^2);
To=(1-Sa*Ro)*T;

fprintf('\nTo is = %0.3f, Ro is = %0.3f\n',To,Ro)
```

```
To is = 0.284, Ro is = 0.481
```

Part c)

filename = 'Capture.txt'; delimiterIn = ','; headerlinesIn = 1; A = importdata(filename,delimiterIn,headerlinesIn);

figure semilogx(A.data(:,1),A.data(:,2))

title('Downward emissivity as a function of W_l','fontsize',20) xlabel('Liquid Water Path (g m^-^2)','fontsize',15) ylabel('Downward Emissivity \epsilon','fontsize',15) hold on x=WL*ones(size(A.data(:,1))) plot(x,A.data(:,2),'k') ylim([0 1.1]); hold off

```
emmisivity=1-exp(-0.158*Wl);
```

Part d) Solar heating rate K/day

```
dT_dt=(1/(rhoa*cp))*(((SctD-SctU)-(ScbU-ScbD))/(z))*(3600*24)
```

```
dT_dt =

   39.4812
```

Part d) Infared heating rate K/day

```
dT_dt=(1/(rhoa*cp))*(((LctD-LctU)-(LcbU-LcbD))/(z))*(3600*24)
```

```
dT_dt =

  -12.5518
```

Published with MATLAB® R2014a